

Electron Transport through CO Studied by Gold Break-Junctions in Nonpolar Liquids

D. den Boer,^{*,†} M. J. J. Coenen,[†] M. van der Maas,[†] T. P. J. Peters,[†] O. I. Shklyarevskii,^{†,‡} J. A. A. W. Elemans,[†] A. E. Rowan,[†] and S. Speller[†]

Institute for Molecules and Materials, Radboud University of Nijmegen, Heyendaalseweg 135, NL-6525 AJ Nijmegen, The Netherlands, and B. Verkin Institute for Low Temperature Physics & Engineering, National Academy of Science of Ukraine, 47 Lenin Av., 61103 Kharkov, Ukraine

Received: June 2, 2009; Revised Manuscript Received: July 10, 2009

We used the mechanically controlled break-junction technique to observe the conductance through carbon monoxide molecules in several nonpolar liquids (toluene, heptane, cyclohexane). CO molecules bridge the electrodes prior to the break, causing the displacement of the first peak in the conductance histograms from ~ 1.0 to 1.1 – 1.15 of the quantum conductance unit ($G_0 = 2e^2/h$). After the break, these molecules remain attached to the electrodes and a peak related to the conductance through a CO molecule appears at 0.2 – $0.3 G_0$.

Introduction

Over the past decade, electrical transport through single molecules has been studied with a number of different techniques, described in detail in recent reviews.^{1–3} Those studies are motivated by prospects of the possibility to build electronic devices on the basis of organic molecules. The significant part of the measurements of molecular conductance was done by using either mechanically controllable break-junctions (MCBJs)^{4–7} or modified STM setups working in organic solvents.^{8–10} The latter are adjusted in such a way that they are similar to the break-junction technique with respect to the repeated connection and disconnection of the tip and sample electrodes. This technique is more flexible in the choice of electrode materials and molecules (and has the additional option of a surface scan) and is therefore often used in spite of its drawbacks as compared to the “true” break-junction technique. The cleanliness of the tip and sample surfaces differs from freshly broken surfaces of MCBJs, and ambient or organic solvent environments have far more contaminants when compared to cryogenic UHV. Ill-controlled cleanliness of the surface and environment can be responsible for the large scattering of data (with a factor from 2 to 50) presented by different groups.^{11,12} The number of articles where molecular conductance was studied with MCBJs in a liquid environment is still very limited.^{13,14}

Here, we report that freshly broken surfaces of the electrodes of MCBJs are sensitive to water and dissolved gases. Even micromoles of these compounds dissolved in the nonpolar liquids already influence the measurements. Therefore, special precautions must be taken with regard to the purification including dehydration and degassing of the solvents. The presence of small quantities of carbon monoxide in toluene, cyclohexane, heptane, and some other nonpolar liquids results in chemisorption of CO molecules on the surface of the gold electrodes at room temperature. In this case, the conductance histograms show an additional peak at 0.2 – $0.3 G_0$, related to the conductance through carbon monoxide molecules bridging the electrodes. A large concentration of CO in the solvent results

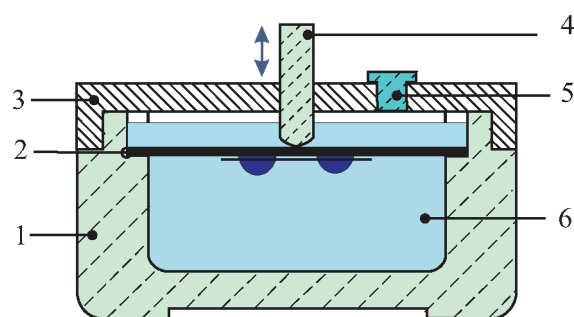


Figure 1. Experimental arrangement: 1, quartz glass cell; 2, sample mounting; 3, Teflon lid; 4, sliding glass piston; 5, opening for changing the content of the cell; 6, solvent.

in the deterioration of the conductance histograms as the entire surface of the electrodes is “contaminated” by chemisorbed carbon monoxide. At the same time, we did not find any influence of dissolved oxygen on the conductance histograms of gold.

Experimental Section

In our experiments, we used a standard MCBJ technique with a conventional type of sample mounting (a notched 125μ wire) described elsewhere.¹⁵ For the flexible bending beam, we used chemically inert bidirectional ($0/90^\circ$) carbon-fiber (CFK) plates of 0.55 mm thickness with excellent elastic properties. A wire was glued on the top of the bending beam with Stycast 2850 FT hard epoxy and cured at 110°C for at least 3 – 4 h. After that, the sample was sonically cleaned in isopropanol, rinsed in ethanol, and afterward sonically cleaned and stored (for days or even weeks) in the solvent under investigation of HPLC grade, without further purification. There were no signs of solvent contamination related to the sample.

Conductance measurements were performed in the quartz glass liquid cell (1) presented in Figure 1. It was hermetically closed with the Teflon lid (3). This allows one to work with volatile solvents for at least 48 – 72 h. The vertical motion from the step-motor and piezo drive was transferred within the cell by the sliding glass piston (4). One more opening in the lid (5), normally tightly closed, was used for changing the content of

* To whom correspondence should be addressed. E-mail: d.denboer@science.ru.nl.

[†] Radboud University of Nijmegen.

[‡] National Academy of Science of Ukraine.

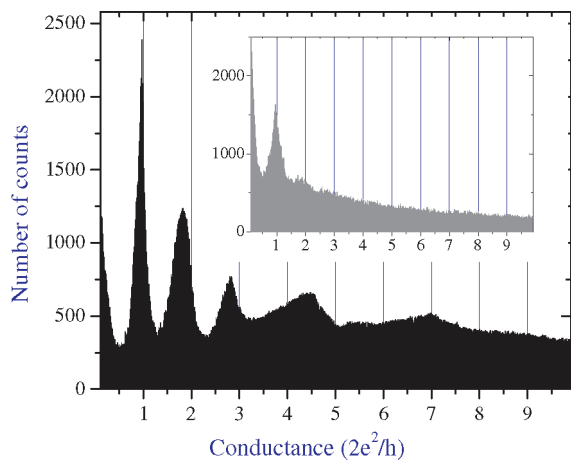


Figure 2. Conductance histogram measured in nondistilled *n*-heptane immediately after the break. The inset shows results for the same sample taken 4 h later.

the cell during measurements. Special care was taken with regard to the cleanliness of the cell and Teflon lid.

Using the traditional sample mounting instead of lithographically made break-junctions has a very important advantage. The aspect ratio (ratio between the vertical motion perpendicular to the MCBJ axis and the distance z between the electrodes) is only around 300–1000 instead of 10^5 . This gives us the possibility of using a standard piezodriver instead of a slow mechanical screw^{13,14} for repeated connection–disconnection cycles, and this allows for a much faster collection of statistical data. The latter is especially important if properties of the electrode surfaces or solvent change during the measurements. Conductance traces were recorded with an AT-MIO-16XE-50 or 6036E National Instruments data acquisition board at sampling rates of 20 000–100 000 points/s. Normally, we used 5000–10 000 individual conductance traces for building up the conductance histograms discussed below, with a bin size of 0.01 G_0 on the linear scale and 100 bins/decade on the logarithmic scale.

In our measurements, we used different nonpolar liquids including *n*-heptane, toluene, cyclohexane, 1,4-dioxane, and some other solvents. The results for all solvents are very similar, and in this article, the presented data is mostly for toluene (one of the most frequently used solvents in experiments with molecular junctions; e.g., see refs 16 and 17).

Results and Discussion

Conductance histograms of coinage metals in pure nonpolar liquids are supposed to show no or little difference from those measured under UHV conditions at room temperature. However, it was found that using nondistilled chemicals of commercial grade (Sigma-Aldrich, Fluka) often led to gradual degradation (on the time scale of hours) of the conductance histograms of Au (Figure 2). Ag and Cu samples did not yield any reasonable data at all, as this degradation occurs on the time scale of minutes.

The gradual deterioration with time or after taking a certain number of conductance curves (connection–disconnection cycles) was also mentioned in refs 18 and 19 among others.

After additional distilling of the solvents, using the standard procedures of removing water with calcium hydride (CaH_2) or sodium metal, we were able to measure Au samples for at least 48–72 h without any detectable changes. The typical conductance histogram measured for Au in distilled toluene is presented

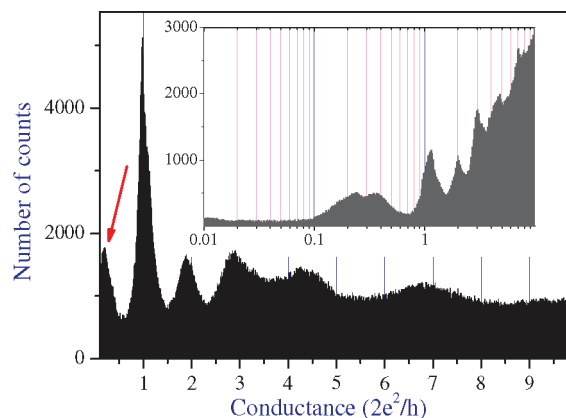


Figure 3. Conductance histogram for gold in distilled toluene. The arrow shows the appearance of a new peak below one quantum of conductance. Inset: conductance histogram for the traces with steps (see Figure 4) in the range 0.1–0.4 G_0 (about 20% of data set).

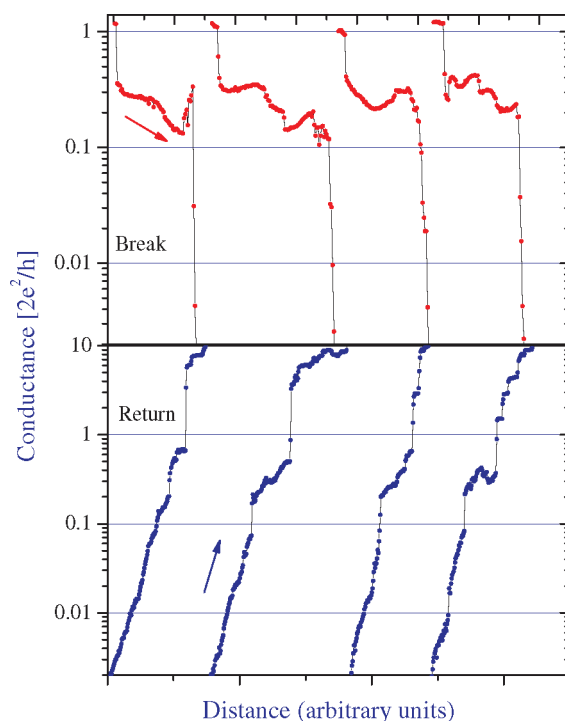


Figure 4. Upper panel: individual conductance traces with steps in the range 0.2–0.4 G_0 from the histogram in the inset of Figure 3. Lower panel: conductance traces plotted as a function of the distance between electrodes on their approach.

in the upper panel of Figure 3 and shows a clear peak (in some cases, a pronounced shoulder) centered between 0.2 and 0.4 G_0 , indicated by the arrow (one quantum unit $G_0 = 2e^2/h$, $1/G_0 \approx 12.9$ k Ω). Only part of the individual conductance traces display steps in this range, which can be selected with a simple program by choosing curves with a maximal number of points in the range of interest. The conductance histogram for the selected traces (approximately 20% of all collected data) is presented on a logarithmic scale in the inset of Figure 3 and displays a clear feature with two maxima. Note that the position of the peak corresponding to the single-atom contact for Au in this histogram is shifted from 0.98–0.99 G_0 to 1.12 G_0 .

The upper panel in Figure 4 shows a few individual conductance traces from the histogram presented in the inset of Figure 3. The conductance steps are not smooth and display chaotic changes in G . The estimated length of the conductance

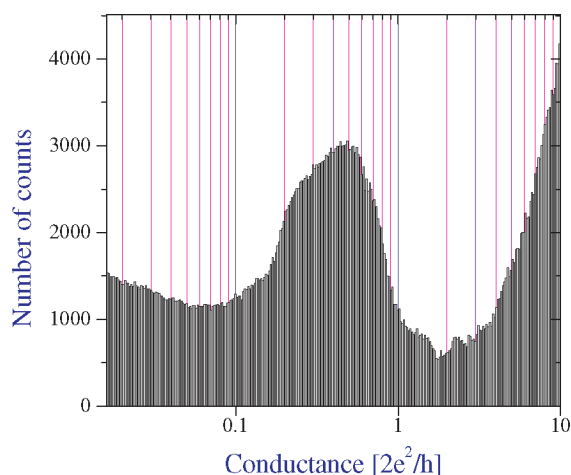


Figure 5. Conductance histogram of the return traces for gold in distilled toluene.

steps is between 0.5 and 1.5 Å (assuming that the work function of Au is reduced to 4.0–4.5 eV by the adsorbed species).

The presence of molecules adsorbed on the surface of the electrodes can be detected by distance tunneling spectroscopy (DTS), by measuring the dependence of the conductance curves on the distance between the electrodes during the approach to the tunneling regime. The effect of adsorbed atoms and molecules on electron tunneling was observed for the first time for He,²⁰ water (using the STM technique),²¹ and recently for hydrogen molecules physisorbed on the surface of some transition metals.²² Individual tunneling $G(z)$ curves (where z is the distance between electrodes) are presented in the lower panel of Figure 4. For statistical analysis of the data, we used the histogram technique. The typical histograms for distilled toluene for the *return traces* are presented in Figure 5. The well-pronounced peak in this histogram (as well as the plateaus in the $G(z)$ curves) indicate the presence of chemically adsorbed molecules on the surface of the gold electrodes.

It should be noted that in spite of the clear conductance steps observed on the individual traces in the range 1–10 G_0 the return conductance histograms for gold are practically featureless, in some cases showing only weak features related to the atomic shell effect. This is in sharp contrast with data for measurements in cryogenic UHV.²³ This effect is totally unexpected and can probably be explained by the viscosity of the liquids being enhanced at nanometer electrode separation.²⁴

Judging from the return traces, the size of the chemisorbed molecules is small. In the absence of any solid theoretical background, we made the rough estimation from the length of “plateaus” on conductance curves which leads to a value below 0.3 nm. This makes the gases dissolved in nonpolar liquids the most probable candidates. The next logical step was the refinement of already distilled solvents. This was done by a degassing procedure of three freeze–pump–thaw cycles resulting in a further improvement of the Au conductance histograms with no sign of additional peaks below 1 G_0 (Figure 6). The number of conductance traces with steps, found between 0.1 and 0.4 G_0 , falls below 0.5%. The increase in the relative intensity of the single-atom peak with respect to the other features in the histograms (including peaks related to the atomic shell effect in gold around 4.5, 7, and 9.5 G_0)²⁵ and the decrease of its half-width after the degassing procedure indicate the decrease of surface contaminations.

These results strongly suggest that the reason for the appearance of the new features in the histogram of the distilled

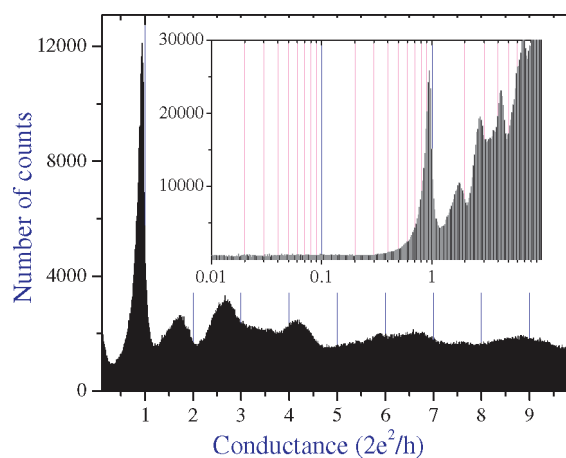


Figure 6. Conductance histogram for gold after degassing the toluene. Inset: this histogram on a logarithmic scale.

nonpolar liquids is related to dissolved gases. Two likely candidates in our case are carbon monoxide and oxygen. It is well-known that CO molecules readily react with transition metals. According to the Blyholder model,²⁶ charge is transferred from the 5σ orbital to the d band of the metal for the CO molecules that are chemisorbed in the linear geometry (M–C–O). This is accompanied by the “back-donation” of this atom’s d orbital electron density into the unoccupied CO $2\pi^*$ antibonding orbital. Such a so-called “push–pull” bond is quite strong.²⁷

For gold, however, the d band is filled and below the Fermi level. Therefore, only the back-donation from the 5d or 6s level into the molecule’s CO $2\pi^*$ antibonding orbital can contribute to the binding to gold. On the bulk gold, chemisorption is weak and occurs only at low temperatures. The case of nanoparticles²⁸ and clusters^{29–32} is different. According to DFT calculations, these particles have a higher concentration of states with d character than bulk metals. They also have a stronger bonding of CO, because of the donation from the 3σ orbital into residual d level vacancies. Gold nanowires (and especially single-atom nanochains with a coordination number of 2) could be even more reactive.³³ Chemisorption of CO at room temperature was observed on clusters³⁴ and surfaces with low coordination number.³⁵

In the case of a CO molecule chemisorbed in the linear geometry, the only expectation is the deterioration of the conductance histograms because of contamination of the surfaces of the electrodes. To measure the conductance through the molecule, it has to be attached to two terminals. Indeed, carbon monoxide can also be chemisorbed in bridge form, connecting two neighboring gold atoms. The carbon atom must then be rehybridized to an sp^2 configuration with three σ bonds in the plane. The bridge form is energetically less favorable than the linear one. Nevertheless, calculations made in ref 36 for CO adsorption on gold with low-coordinated sites demonstrated that the situation in which a CO molecule is bridging two atoms can be stable at certain surfaces.

To prove that the new feature observed in the gold conductance histograms is related to the conductance through the CO molecule, we dissolved spectroscopically pure CO in the preliminary distilled and degassed toluene by leading this gas through the liquid for 2–5 h. The solubility of carbon monoxide in toluene at room temperature and atmospheric pressure is about 7 mM,³⁷ and this proved too high for our measurements. The conductance histograms are almost featureless and display only the remnants of the single-atom peak (Figure 7). This indicates

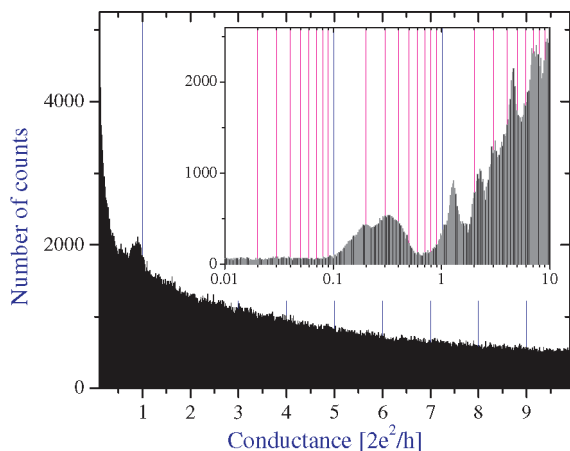


Figure 7. Conductance histogram for gold in toluene saturated with carbon monoxide. Inset: conductance histogram measured in diluted solution for the traces with steps in the range $0.1\text{--}0.4 G_0$ (about 20% of data set).

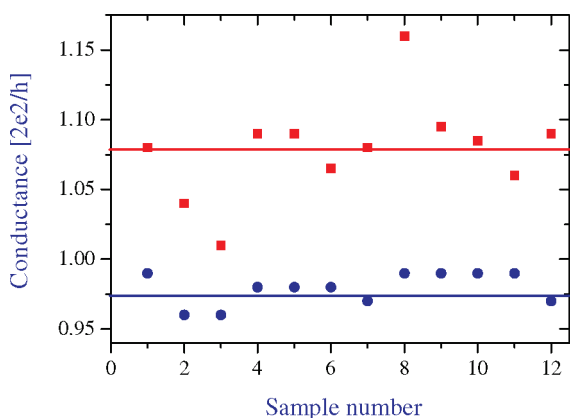


Figure 8. Position of the peak related to the single-atom contact between gold electrodes in the original conductance histograms (circles) and in the histograms constructed from selected traces with the steps in the range $0.2\text{--}0.4 G_0$ (squares). The first six points are related to the measurements in toluene, while the last six are related to the measurements in cyclohexane.

a strong interaction between carbon monoxide and the surface of the electrodes.

To reduce the coverage of the electrode surfaces with chemisorbed carbon monoxide, we used a diluted solution of CO (100 or more parts of degassed toluene mixed with 1 part of toluene saturated with CO). For such a concentration, we were again able to observe the features at $0.2\text{--}0.3 G_0$ (inset in Figure 7, conductance histogram for the selected traces with steps in the range $0.1\text{--}0.4 G_0$). Though it is difficult to accurately estimate the actual concentration of carbon monoxide in the solvent, the Au break-junctions are sensitive to the presence of the CO for even less than $10 \mu\text{M}$.

Comparison of the single-atom peak position in the original conductance histograms (raw data) and the position of the relevant peak in histograms for curves selected by a program shows that in the latter case there is a shift to the values exceeding $1 G_0$. The differences between the positions of the mentioned peaks vary from sample to sample and are in the range $0.03\text{--}0.15 G_0$; their averaged value is close to $0.1 G_0$ (see Figure 8). As the conductance limit through a single-atom gold contact cannot be higher than $1 G_0$, this effect can be explained by suggesting that the CO molecule is already adsorbed on the surface of the gold nanowire prior to the break. The case of the gold nanowire with the carbon monoxide

molecule bridging two atoms in the short single-atom gold chain will result in the observed increase of conductance. After the disconnection of the gold atoms, the CO molecule remains attached between two electrodes and we measure the conductance through this molecule, which in our case is equal to $0.3 \pm 0.1 G_0$.

It should be noted that the difference in conductance for the “clean” single-atom contact and the one bridged by a CO molecule is considerably less than the measured conductance through the molecule. The possible explanation is that conductance of the CO molecule stretched between the electrodes is higher due to the changes in its electronic structure caused by deformation and changes in the adsorption geometry.

In the nonpolar liquids, it was only possible to observe the conductance through the carbon monoxide molecule at relatively small concentrations of CO (less than 0.1 mM) and when the surface was clean enough. The cleanliness of the gold surface is indicated by a high intensity of the first peak in the gold conductance histograms, i.e., the possibility of pulling (short) single-atom nanochains.

Our data for the conductance through a carbon monoxide molecule in nonpolar liquids differ from the conductance of CO between electrodes of Pt, Ni, Cu, and Au MCBJs in UHV reported in ref 38. In all of those cases, the relevant peak in the conductance histograms was very close to $0.5 G_0$. This difference can be explained by the difference in the experimental conditions; in ref 38, all measurements were done in cryogenic vacuum at 4.2 K . At low temperatures, the bonding of CO to the gold surface is much stronger and this can be the cause of the higher value of conductance.

The features in the conductance histograms related to carbon monoxide are most often visible as two peaks (visible on a logarithmic scale). The possible reason for such a shape can be the dependence of the bond strength (and therefore conductance) on the coordination number for gold atoms bridged by a CO molecule.

Additional distilling and degassing of the solvents gives us the opportunity to measure a silver MCBJ for a sufficiently long period of time. Silver has lower-lying d states and less s–d hybridization than gold. At some occasions, we were able to observe the additional features in the conductance histograms around $0.2\text{--}0.3 G_0$, with values of considerably lower amplitude than those for gold junctions.

We also measured gold MCBJs in toluene and cyclohexane saturated (after preliminary distilling and degassing) with oxygen. No evidence of an interaction of O_2 with the surface of the electrodes was found, which is in agreement with the fact that dissociation and chemisorption of oxygen does not occur on gold nanoparticles and clusters.²⁷

In conclusion, we measured conductance through a single molecule of carbon monoxide using MCBJs operating in nonpolar liquids with dissolved CO gas. Our experiments also show the possibility to study the interaction of gases with metallic surfaces using nonpolar liquids as a neutral environment.

Acknowledgment. The authors thank J. Hermsen and J. Gerritsen for invaluable technical assistance and J. M. van Ruitenbeek and R. J. M. Nolte for stimulating discussions. Part of this work was supported by the Nanotechnology network in The Netherlands NanoNed, by the Ministry of Economic Affairs and the Stichting voor Fundamenteel Onderzoek der Materie (FOM) which is financially supported by the Nederlandse Organisatie voor Wetenschappelijk Onderzoek (NWO). O.I.S. wishes to thank the FOM and NWO for a visitor’s grant.

References and Notes

- (1) Akkerman, H. B.; de Boer, B. *J. Phys.: Condens. Matter* **2008**, *20*, 013001.
- (2) Selzer, Y.; Allara, D. L. *Annu. Rev. Phys. Chem.* **2006**, *57*, 593.
- (3) Chen, F.; Hihath, J.; Huang, Z.; Li, X.; Tao, N. *J. Annu. Rev. Phys. Chem.* **2008**, *58*, 535.
- (4) Chen, J.; Reed, M. A.; Rawlett, A. M.; Tour, J. M. *Science* **1999**, *286*, 1550.
- (5) Smit, R. H. M.; Noat, Y.; Untiedt, C.; Lang, N. D.; van Hemert, M. C.; van Ruitenbeek, J. M. *Nature* **2002**, *419*, 906.
- (6) Csonka, Sz.; Halbritter, A.; Mihaly, G.; Jurdik, E.; Shklyarevskii, O. I.; Speller, S.; van Kempen, H. *Phys. Rev. Lett.* **2004**, *93*, 016802.
- (7) van Ruitenbeek, J. M.; Scheer, E.; Weber, H. In *Introducing Molecular Electronics*; Cuniberti, G., Fagas, G., Richter, K., Eds.; Springer Lecture Notes in Physics; Springer: Heidelberg, Germany, 2005; pp 253–274.
- (8) Xu, B.; Tao, N. *J. Science* **2003**, *301*, 1221.
- (9) Haiss, W.; Nichols, R. J.; van Zalinge, H.; Higgins, S. J.; Bethell, D.; Schiffrin, D. *J. Phys. Chem. Chem. Phys.* **2004**, *6*, 4330.
- (10) Venkataraman, L.; Klare, J. E.; Tam, I. W.; Nuckolls, C.; Hybertsen, M. S.; Steigerwald, M. L. *Nano Lett.* **2006**, *6*, 458.
- (11) Lindsay, S. M.; Ratner, M. *Adv. Mater.* **2007**, *19*, 23.
- (12) Ulrich, J.; Esrail, D.; Pontius, W.; Venkataraman, L.; Millar, D.; Doerrer, L. H. *J. Phys. Chem. B* **2006**, *110*, 2462.
- (13) Gonzáles, M. T.; Wu, S.; Huber, R.; van der Molen, S. J.; Schönenberger, C.; Calame, M. *Nano Lett.* **2006**, *6*, 2238.
- (14) Huber, R.; Gonzáles, M. T.; Wu, S.; Langer, M.; Grunder, S.; Horhoiu, V.; Mayor, M.; Bryce, M. R.; Wang, C.; Jitchati, R.; Schönenberger, C.; Calame, M. *J. Am. Chem. Soc.* **2008**, *130*, 1080.
- (15) Agrait, N.; Levy Yeyati, A.; van Ruitenbeek, J. M. *Phys. Rep.* **2003**, *377*, 8103.
- (16) He, J.; Chen, F.; Li, J.; Sankey, O. F.; Terazono, Y.; Herrero, C.; Gust, D.; Moore, T. A.; Moore, A. L.; Lindsay, S. M. *J. Am. Chem. Soc.* **2005**, *127*, 1384.
- (17) Huang, Z.; Chen, F.; Bennett, P. A.; Tao, N. *J. Am. Chem. Soc.* **2007**, *129*, 13225.
- (18) Millar, D.; Venkataraman, L.; Doerrer, L. H. *J. Phys. Chem. C* **2007**, *111*, 17635.
- (19) Long, D. P.; Lazorcik, J. L.; Mantooth, M. A.; Moore, M. H.; Ratner, M. A.; Troisi, A.; Yao, Y.; Cizek, J. W.; Tour, J. M.; Shashidhar, P. *Nat. Mater.* **2006**, *5*, 901.
- (20) Keijsers, R. J. P.; Voets, J.; Shklyarevskii, O. I.; van Kempen, H. *Phys. Rev. Lett.* **1996**, *76*, 1138.
- (21) Hugelmann, M.; Schindler, W. *Surf. Sci.* **2003**, *541*, L643.
- (22) den Boer, D.; Shklyarevskii, O. I.; Elemans, J. A. A. W.; Speller, S. *Phys. Rev. B* **2008**, *77*, 165423.
- (23) Yanson, I. K.; Shklyarevskii, O. I.; Csonka, Sz.; van Kempen, H.; Speller, S.; Yanson, A. I.; van Ruitenbeek, J. M. *Phys. Rev. Lett.* **2005**, *95*, 256806.
- (24) Li, T. D.; Gao, D.; Szoszkiewicz, R.; Landman, U.; Riedo, E. *Phys. Rev. B* **2005**, *75*, 115415.
- (25) Mares, A. I.; Otte, A. F.; Soukiassian, L. G.; Smit, R. H. M.; van Ruitenbeek, J. M. *Phys. Rev. B* **2004**, *70*, 073401.
- (26) Blyholder, G. *J. Chem. Phys.* **1964**, *68*, 2772.
- (27) Bond, G. C.; Louis, C.; Thompson, D. T. *Catalysis in gold*; Imperial College Press: Singapore, 2006.
- (28) Lopez, N.; Nørskov, J. K. *J. Am. Chem. Soc.* **2002**, *124*, 11262.
- (29) Phala, N. S.; Klatt, G.; van Steen, E. *Chem. Phys. Lett.* **2004**, *395*, 33.
- (30) Yuan, D. W.; Zenga, Z. *J. Chem. Phys.* **2004**, *120*, 6574.
- (31) Häkkinen, H.; Moseler, M.; Landman, U. *Phys. Rev. Lett.* **2002**, *89*, 033401.
- (32) Sanchez, A.; Abbet, S.; Heiz, U.; Schneider, W. D.; Häkkinen, H.; Barnett, R. N.; Landman, U. *J. Phys. Chem. A* **1999**, *103*, 9573.
- (33) Bahn, S. R.; Lopez, N.; Nørskov, J. K.; Jacobsen, K. W. *Phys. Rev. B* **2002**, *66*, 081405.
- (34) Veldeman, N.; Lievens, P.; Andersson, M. *J. Phys. Chem. A* **2005**, *109*, 11793.
- (35) Gottfried, J. M.; Schmidt, K. J.; Schroeder, S. L. M.; Christmann, K. *Surf. Sci.* **2003**, *536*, 206.
- (36) Yim, W. L.; Nowitzki, T.; Necke, M.; Schnars, H.; Nickut, P.; Biener, J.; Biener, M.; Zielasek, V.; Al-Shamery, K.; Kluner, T.; Baumer, M. *J. Phys. Chem. C* **2007**, *111*, 445.
- (37) Field, L. R.; Wilhelm, E.; Battino, R. *J. Chem. Thermodyn.* **1974**, *6*, 237.
- (38) Kiguchi, M.; Djukic, D.; van Ruitenbeek, J. M. *Nanotechnology* **2007**, *18*, 035205.

JP905171S